



Growth and Characterization of Arsenic-Doped CdTe_{1-x}Se_x Single Crystals Grown by the Cd-Solvent Traveling Heater Method

AKIRA NAGAOKA ^{1,5}, KENSUKE NISHIOKA,¹ KENJI YOSHINO,²
DARIUS KUCIAUSKAS,³ and MICHAEL A. SCARPULLA^{4,6}

1.—Research Center for Sustainable Energy and Environmental Engineering, University of Miyazaki, Miyazaki 889-2192, Japan. 2.—Department of Applied Physics and Electronic Engineering, University of Miyazaki, Miyazaki 889-2192, Japan. 3.—National Renewable Energy Laboratory (NREL), Golden, CO 80401, USA. 4.—Department of Materials Science and Engineering, University of Utah, Salt Lake City, UT 84112, USA. 5.—e-mail: nagaoka.akira.m0@cc.miyazaki-u.ac.jp. 6.—e-mail: mike.scarpulla@utah.edu

The photovoltaic performance of CdTe solar cells is mainly limited by low doping and short minority carrier lifetime. Group-V element doping and Se-alloying have a significant impact on tuning these fundamental CdTe properties. In this paper, we report the growth of *p*-type As-doped, Cd-rich CdTe_{1-x}Se_x single crystals using metallic Cd as the solvent in the traveling-heater method. The structural and electrical properties of CdTe_{1-x}Se_x are examined for different Se concentrations. CdTe_{1-x}Se_x single crystals ($0 \leq x \leq 0.5$) with zincblende structure indicate homogeneous composition. The 10^{17} cm^{-3} As-doping activation efficiency can be maintained at close to 50% for $x \leq 0.2$. Se alloying leads to bulk minority carrier lifetime exceeding 30 ns for samples doped near 10^{17} cm^{-3} . These results help us to overcome the current roadblocks in device performance.

Key words: CdTeSe, group-V doping, minority carrier lifetime, photovoltaics, solar cells, single crystals

INTRODUCTION

Cadmium telluride (CdTe) photovoltaic (PV) modules are relatively easy to produce at low cost, making them one of the most competitive commercially available PV technologies. The current world-record PV cell has power conversion efficiency of 22.1%, which is well below the theoretical limits.¹ Achieving improved efficiency without increasing the production costs will make PV generation more competitive with fossil fuels. The practical strategy for higher efficiency is through improvement of open-circuit voltage (V_{OC}) and short-circuit current (J_{SC}).

It was recently discovered that group-V element doping (P, As, Sb, or Bi) and Cd-rich composition are key technologies for increasing V_{OC} , and these results were attributed to high *p*-type doping and long minority carrier lifetime. PV devices fabricated with P-doped CdTe single crystals as absorbing layer and with Cd-rich composition could result in hole concentration of $\sim 10^{17} \text{ cm}^{-3}$, minority carrier lifetime of several hundreds of a nanosecond, and V_{OC} exceeding 1 V.² However, it is difficult to obtain group-V doping higher than 10^{17} cm^{-3} because doping efficiency typically decreases with higher dopant incorporation (above $\sim 10^{16} \text{ cm}^{-3}$).³⁻⁵ The origin of this doping limit has not been established, but theoretical studies suggest that it may be caused by the formation of self-compensating AX center or defect complex.³⁻⁶ The AX center is formed due to a large lattice relaxation of the substitutional

(Received January 8, 2020; accepted July 17, 2020; published online August 2, 2020)

dopant, which results in conversion to a donor state.^{3,5} It was recently reported that in situ As-doping in polycrystalline thin film CdTeSe PV devices achieved greater than 20% power conversion efficiency, but dopant activation remained low (2–4%).⁷

We have reported that CdTe doping with As leads to a shallow acceptor, presumably As_{Te} , with activation energy of 70 meV, and we also saw evidence consistent with AX behavior such as persistent photoconductivity.⁸ So far, we have obtained close to 50% As doping activation at hole concentration of 10^{17} cm^{-3} , hole mobility $> 70 \text{ cm}^2/\text{Vs}$, bulk lifetime $> 30 \text{ ns}$, and $V_{OC} > 900 \text{ mV}$ in As-doped CdTe single-crystal solar cells.^{8–10}

On the other hand, CdTe alloying with Se ($CdTe_{1-x}Se_x$) has attracted strong interest as a means for improving J_{SC} , because lower bandgap leads to increased absorption in the long-wavelength part of the spectrum. Bandgap tuning through alloying is widely used in PV. For example, high-efficiency $Cu(In_xGa_{1-x})Se_2$ (CIGS) absorbers employ bandgap grading by controlled variation of In/Ga composition.¹¹ Alloying CdTe at the cation site for bandgap grading is not practical, because the bandgap always increases when Cd is substituted by isovalent Zn,¹² and it is undesirable to alloy with HgTe given the toxicity of Hg. Thus, substituting the anion site of CdTe is the only feasible method for reducing the bandgap. Even though the bandgap values of CdS ($E_g = 2.48 \text{ eV}$) and CdSe ($E_g = 1.73 \text{ eV}$) are both larger than that of CdTe ($E_g = 1.48 \text{ eV}$) at room temperature,¹³ alloying CdS or CdSe with CdTe can effectively reduce its bandgap due to the large bowing effect.¹⁴ The low solubility of S in CdTe has been confirmed by previous theoretical and experimental studies.^{14,15} Alloying CdTe with CdSe seems to be the best way to effectively reduce the bandgap, and experimental studies have demonstrated that $CdTe_{1-x}Se_x$ enables the enhancement of J_{SC} .^{16–18}

In this paper, we combine the two approaches in order to develop more efficient CdTe solar cells: group-V doping and alloying with Se. We have previously grown high-quality As-doped Cd-rich CdTe single crystals from metal Cd solvent near thermodynamic equilibrium using the traveling heater method (THM).¹⁹ In this study, we investigated the growth of group-V doped Cd-rich $CdTe_{1-x}Se_x$ single crystals using the THM. It is now becoming clearer how the formation of the $CdTe_{1-x}Se_x$ alloy may affect the group-V doping and physical properties, and this report proposes some possible answers to these questions.

EXPERIMENTAL PROCEDURE

Crystal growth was carried out at the University of Miyazaki. First, all feed polycrystalline ingots of $CdTe_{1-x}Se_x$ with $x = 0–0.6$ were prepared by melting and reacting elemental Cd (99.999%, Kojundo Chemical Laboratory Co., Ltd.), Te (99.999%,

Kojundo Chemical Laboratory Co., Ltd.) and Se (99.9999%, Osaka Asahi Metal Mfg. Co., Ltd.) shots from the same batch, which were chemically etched to remove surface oxide. Cd was etched with HCl solution for 60 s and then rinsed in ultrapure 18 MOhm water. Te was etched in H_2SO_4 solution for 5 min and then rinsed in ultrapure water. The prescribed amounts of elements were sealed off in an evacuated carbon-coated quartz ampoule with 2 mm wall thickness and 9 mm inner diameter under high vacuum of $2 \times 10^{-4} \text{ Pa}$ by using a liquid N_2 -trapped diffusion pump. In a vertical furnace, the sealed ampoule was heated at $150^\circ\text{C}/\text{h}$ to 650°C and held at this temperature for 24 h to react the constituents and prevent explosion from the Cd or Se overpressure. The sealed ampoule was then heated at $50^\circ\text{C}/\text{h}$ to 1100°C and held at this temperature for 24 h to complete the reaction and ensure homogenization. The ampoule was then removed from the vertical furnace and allowed to cool rapidly in air. The feed polycrystalline $CdTe_{1-x}Se_x$ ingot, Cd solvent and Cd_3As_2 dopant shot (99.999%, American Elements) were loaded into a carbon-coated quartz ampoule with 10 mm inner diameter and 2 mm wall thickness. The ampoule was sealed under high vacuum ($2 \times 10^{-4} \text{ Pa}$) and then lowered through the hot zone of the THM furnace at 1–2 mm/day at a temperature gradient of $30^\circ\text{C}/\text{cm}$ for crystal growth. Grown crystals were cut with a diamond blade and polished mechanically with $0.1 \mu\text{m}$ Al_2O_3 paste and then etched with a 5% $Br_2/\text{Methanol}$ solution for 5 min to remove saw and polishing damage before conducting measurements.

The structural properties were measured by powder x-ray diffraction (XRD; X'Pert PRO, PANalytical). The XRD experiment was performed at 40 kV and 40 mA using a Cu-K α radiation source with a step width of 0.01° . The XRD patterns were calibrated with a silicon powder (NIST SRM 640d) to observe the peak shift. The average elemental composition of the samples was determined using scanning electron microscopy (SEM; S-5500, Hitachi) and energy-dispersive x-ray spectroscopy (EDS). EDS measurements were calibrated by a stoichiometric CdTe reference crystal (AcroRad Co., Ltd.). The As dopant and impurity concentration in the grown crystals was determined by inductively coupled plasma atomic emission spectroscopy (ICP-AES; SPS3520UV, SII NanoTechnology). The nominal As doping concentration was $(1.0–2.0) \times 10^{17} \text{ cm}^{-3}$ in $CdTe_{1-x}Se_x$ samples. Samples were dissolved in a mixed acid containing $1.2 \text{ mol L}^{-1} \text{ HNO}_3$ and $0.3 \text{ mol L}^{-1} \text{ HCl}$. The hole concentration was obtained by Hall effect measurements (ResiTest 8300, TOYO Corporation), performed in a 0.45 T magnetic field in the van der Pauw geometry. For electrical measurements, Ni-W alloy contacts, each with a diameter of 1 mm and thickness of about 200 nm, were deposited by RF sputtering onto the corners of a sample (approximately $5 \text{ mm} \times 5 \text{ mm} \times 1 \text{ mm}$) using shadow-mask, and then, all

samples were annealed at 300°C under 96% N₂–4% H₂ mixed gas for 10 min to form the ohmic contacts. XRD, SEM, EDS, and Hall effect measurements were carried out at the University of Miyazaki. Bulk minority-carrier lifetime was measured by two-photon excitation time-resolved photoluminescence (2PE-TRPL) at the National Renewable Energy Laboratory.²⁰ The laser system provided 1120 nm excitation using 0.3 ps pulses at 1.1 MHz repetition rate.

RESULTS AND DISCUSSION

Structural Properties of CdTe_{1-x}Se_x

The stoichiometric feed polycrystalline CdTe_{1-x}Se_x ($x = 0-0.6$) ingots weighed approximately 10–15 g. In our previous study,¹⁹ Cd-rich CdTe single crystals were grown from 50 mol% Cd solvent at a growth temperature of 950°C through the three zones of the furnace. In this study, the THM growth temperature with increasing Se composition was increased to 1000°C because the melting point of CdTe_{0.5}Se_{0.5} is 20–30°C higher than that of CdTe.²¹ Figure 1 is an image of one CdTe_{0.5}Se_{0.5} ingot in which the Cd solvent zone can be observed.

It is well known that CdTe crystallizes in the cubic zincblende structure, while CdSe crystallizes in the hexagonal wurtzite structure.^{17,21} The two structures are closely related; in both, Cd atoms are surrounded by Te and/or Se atoms in a tetrahedral configuration. The cubic zincblende structure is present at low temperature, with a transition to hexagonal wurtzite structure above 800–1000°C with $0.2 \leq x \leq 0.5$.^{17,21} This transition temperature decreases with increasing Se content, and the hexagonal wurtzite phase is dominant with $x \geq 0.6$.¹⁷ Powder XRD measurements were performed on CdTe_{1-x}Se_x samples with $0.1 \leq x \leq 0.6$, and data are shown in Fig. 2a. The structure was identified as a cubic zincblende structure with higher peak shifting for $0.1 \leq x \leq 0.5$, which is in good agreement with references.^{17,21} In addition,

there is no peak splitting in the dominant positions such as (111), (220) and (311) from the International Centre for Diffraction Data (ICDD) for CdTe (#03-065-1082). This means that a tetragonal distortion is not observed with $0 \leq x \leq 0.5$. Figure 2b shows the XRD patterns for $x = 0.5$ and 0.6 over the angle range $20^\circ \leq 2\theta \leq 30^\circ$, which reveals that the hexagonal wurtzite phase is dominant with $x \geq 0.6$. Only one peak (24.5°) related to cubic structure can be observed for $x = 0.5$ which indicates a uniform solid solution, while there are three peaks for $x = 0.6$ and the dominant 23.3° peak, indicating the hexagonal wurtzite structure. Considering PV device applications, the zincblende structure is desired, while the wurtzite structure is not photoactive.¹⁷ Therefore,



Fig. 1. Example of the resulting CdTe_{0.5}Se_{0.5} ingot grown by Cd solution.

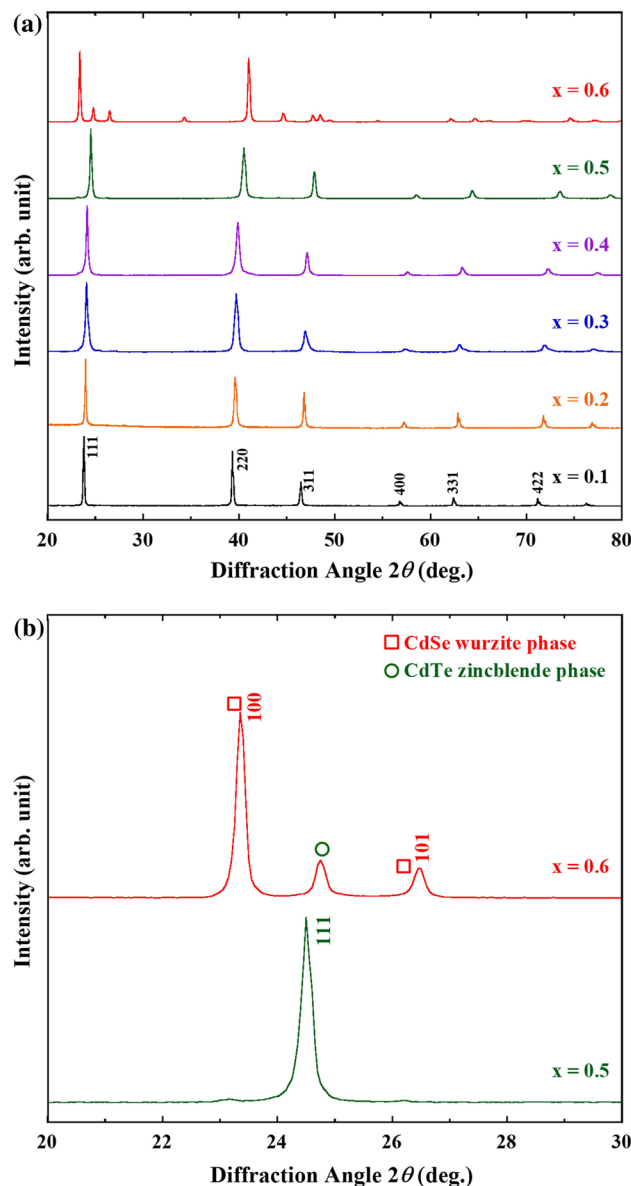


Fig. 2. (a) Powder XRD patterns of CdTe_{1-x}Se_x samples. (b) XRD patterns of $x = 0.5$ and 0.6 over the angle range $20^\circ \leq 2\theta \leq 30^\circ$. ICDD CdTe (#03-065-1082) and CdSe (#01-071-4772) are references.

Table I. Chemical composition of Cd-rich CdTe_{1-x}Se_x single crystals

$x =$	Composition from EDS [at.%]		
	Cd	Te	Se
0	50.32	49.68	—
0.1	50.44	45.47	4.09
0.2	50.38	41.31	8.31
0.3	50.23	35.92	13.85
0.4	50.29	31.32	18.39
0.5	50.34	25.74	23.92
0.6	50.15	20.73	29.12

we focus on samples with $x < 0.6$ in which the cubic structure is dominant.

Table I shows the composition of Cd-rich CdTe_{1-x}Se_x single crystals ($x \leq 0.5$) from EDS measurements made at three points near the edges and at the center of the wafers (mechanically polished and not etched). The uniformity of the composition along the growth direction measured by EDS is shown in Fig. 3 for CdTe_{0.5}Se_{0.5} wafers cut from the growth tip at 5 mm intervals except for the end region. The error bars shown are the standard deviation of these measurements and thus do not reflect the systematic error of the EDS measurement itself. It can be observed that CdTe_{1-x}Se_x crystals appear to be spatially homogeneous and slightly Cd-rich within +0.5 at.%.

Group-V Doping Properties

Group-V doping as As atom and impurity concentrations were determined by ICP-AES. Table II shows the concentrations of impurities which exceed 100 ppb for non-doped CdTe_{1-x}Se_x ($x = 0, 0.5$). Impurities important for solar cells, such as Cu and Cl, were measured at less than 100 ppb.^{22,23} In this study, As concentrations were less than 10^{17} cm^{-3} , as we have reported that in Cd-rich CdTe with activation $> 50\%$, the As doping limit is close to 10^{17} cm^{-3} .¹⁰ The doping activation efficiency (hole concentration p /As doping concentration) versus Se composition (x) is shown in Fig. 4. Our data indicate that high As-doping activation efficiency close to 50% can be maintained up to $x = 0.2$. With increasing Se content, the doping activation decreases to less than 20%. This may be because Cd compounds with a Te anion have a tendency to be p -type, while those with a Se anion have a tendency to be n -type.¹³ We found that p -type conduction can be observed with $0 \leq x \leq 0.5$, which means these Se compositions can be used for absorber bandgap grading. The group-V doping method previously developed for single-

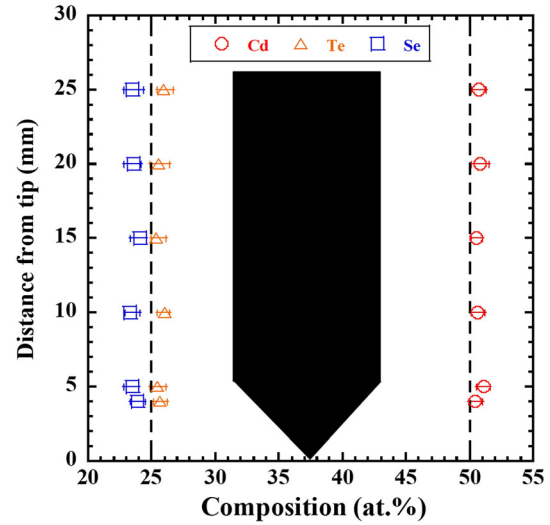


Fig. 3. Chemical composition of non-doped CdTe_{0.5}Se_{0.5} single crystal by EDS along the growth direction.

Table II. Unintentional impurity levels detected by ICP-AES in CdTe_{1-x}Se_x ($x = 0, 0.5$)

Impurity (ppb)	$x = 0$	$x = 0.5$
C	770	830
O	310	340
Mg	450	600
Al	360	220
Si	460	530

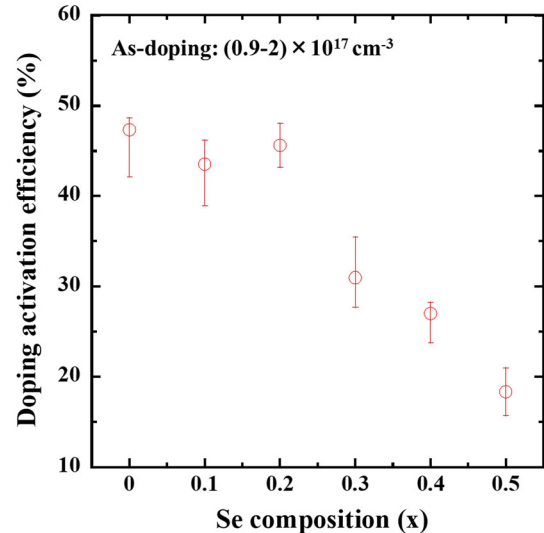


Fig. 4. Doping activation efficiency (hole concentration/measured As concentration) versus Se composition in CdTe_{1-x}Se_x single crystals. As-doping concentration is close to 10^{17} cm^{-3} in all samples.

crystal CdTe could be applied to the CdTeSe compositions.

Bulk Minority Carrier Lifetime

One of the greatest advantages of Se alloying is the improvement of minority carrier lifetime by the passivation of bulk defects in the absorber.¹⁸ In addition, recombination velocity less than 100 cm/s at the Al₂O₃/CdTeSe interface has been reported.²⁴ The bulk lifetime is an important parameter contributing to PV device performance. Typical one-phonon excited TRPL probes rather shallow absorption depths in CdTe because of the large absorption coefficient, which makes such data strongly influenced by surface recombination. 2PE-TRPL using sub-bandgap excitation can be focused > 100 μm from the surface in the bulk crystals, thus avoiding surface recombination effects, which enables the evaluation of bulk carrier lifetimes. The 2PE-TRPL decay curves of non-doped and 10¹⁷ cm⁻³ As-doped Cd-rich CdTe_{1-x}Se_x single crystals ($x = 0, 0.2$) are shown in Fig. 5. Lifetime τ_{TRPL} in the range of several tens of nanoseconds can be obtained from the exponential decay in the latter section of the decay curve. To evaluate and compare recombination lifetime results, we calculate the internal radiative efficiency (IRE) as

$$\text{IRE} = \frac{\tau_{\text{TRPL}}}{\tau_{\text{TRPL}} + \tau_{\text{R}}} = \frac{\tau_{\text{TRPL}}}{\tau_{\text{TRPL}} + 1/Bp}, \quad (1)$$

where $\tau_{\text{R}} = 1/BN_{\text{A}}$ is the radiative lifetime, $B = 1 \times 10^{-10}$ cm³/s is the radiative recombination coefficient (assumed to be the same as in CdTe),²⁵ and N_{A} is the doping concentration. For non-doped samples, we use hole concentration estimated from the first principles analysis on CdTe, $N_{\text{A}} = 1.77 \times 10^{14}$ cm⁻³.²⁶ Data in Fig. 5 indicate IRE = 0.05–0.1% for non-doped and IRE = 13–33% for As-doped CdTe_{1-x}Se_x. We suggest this remarkable > 100-fold increase in radiative efficiency may be associated with highly efficient group-V doping. Our data show that Se atoms play an important role in increasing bulk carrier lifetime and radiative efficiency. Remarkably, the bulk lifetime of the 10¹⁷ cm⁻³ As-doped Se-alloyed sample with 50% activation was measured to be > 30 ns. This combination of group-

V doping under Cd-rich conditions and Se alloying is commensurate with the lifetime in state-of-the-art Cu-doped PV devices.²⁷

CONCLUSION

In this study we report on the growth and characterization of group-V doped Cd-rich CdTe_{1-x}Se_x single crystals from THM. The crystal structure is identified as the cubic zincblende structure $0 \leq x \leq 0.5$, while the hexagonal wurtzite structure is dominant with $x \geq 0.6$. The composition of the non-doped CdTe_{0.5}Se_{0.5} single crystals was homogeneous along the growth and radial directions, and the crystals were found to be slightly Cd-rich. Group-V (arsenic atom) doping activation efficiency has a tendency to be lower with increased Se content. High doping activation close to 50% was obtained in the range of $\sim 10^{17}$ cm⁻³ doping at low Se content. Long minority carrier lifetime of more than 30 ns can be obtained by Se alloying. The combination of group-V doping and Se alloying in CdTe can be used to fabricate PV devices with an increase in both V_{OC} and J_{SC} by introducing bandgap grading in the absorber.

ACKNOWLEDGMENTS

A.N. acknowledges support from the JSPS for a Research Fellow Grant-in-Aid. At NREL, this work is supported by the U.S. Department of Energy's Office of Energy Efficiency and Renewable Energy (EERE) under Solar Energy Technologies Office (SETO) Agreement No. 34350 operated by Alliance for Sustainable Energy, LLC, for the U.S. Department of Energy (DOE) under Contract No. DE-AC36-08GO28308. The views expressed in the article do not necessarily represent the views of the DOE or the U.S. Government.

CONFLICT OF INTEREST

The authors declare that they have no conflict of interest.

REFERENCES

1. M. A. Green, E. D. Dunlop, D. H. Levi, J. H-Ebinger, M. Yoshita, and A. W. Y. H-Baillie, *Prog. Photovoltaics* 27, 565 (2019).
2. J.M. Burst, J.N. Duenow, D.S. Albin, E. Colegrove, M.O. Reese, J.A. Aguiar, C.S. Jiang, M.K. Patel, M.M. Al-Jassim, D. Kuciauskas, S. Swain, T. Ablekim, K.G. Lynn, and W.K. Metzger, *Nat. Energy* 1, 16015 (2016).
3. J.H. Yang, W.J. Yin, J.S. Park, J. Ma, and S.H. Wei, *Semicond. Sci. Technol.* 31, 083002 (2016).
4. J.H. Yang, W.J. Yin, J.S. Park, J. Burst, W.K. Metzger, T. Gessert, T. Barnes, and S.H. Wei, *J. Appl. Phys.* 118, 025102 (2015).
5. T. Ablekim, S.K. Swain, W.J. Yin, K. Zaunbrecher, J. Burst, T.M. Barnes, D. Kuciauskas, S.H. Wei, and K.G. Lynn, *Sci. Rep.* 7, 4563 (2017).
6. D. Krasikov and I. Sankin, *Phys. Rev. Mater.* 2, 103803 (2018).
7. W.K. Metzger, S. Grover, D. Lu, E. Colegrove, J. Moseley, C.L. Perkins, X. Li, R. Mallick, W. Zhang, R. Malik, J. Kephart, C.-S. Jiang, D. Kuciauskas, D.S. Albin, M.M. Al-

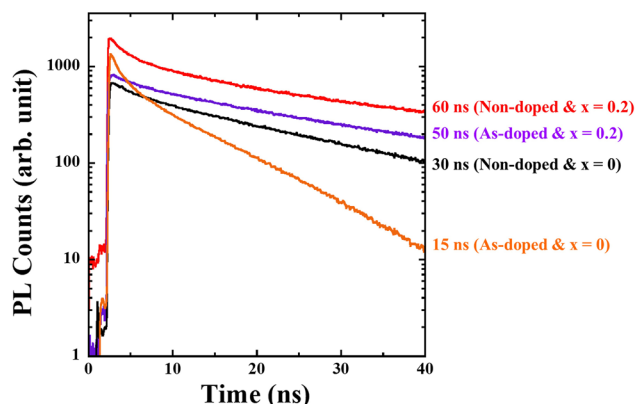


Fig. 5. Normalized 2PE-TRPL decay for bulk lifetime in As-doped CdTe_{1-x}Se_x single crystals ($x = 0, 0.2$).

- Jassim, G. Xiong, and M. Gloeckler, *Nat. Energy* 4, 837 (2019).
8. A. Nagaoka, D. Kuciauskas, and M.A. Scarpulla, *Appl. Phys. Lett.* 111, 232103 (2017).
 9. A. Nagaoka, D. Kuciauskas, J. McCoy, and M.A. Scarpulla, *Appl. Phys. Lett.* 112, 192101 (2018).
 10. A. Nagaoka, K. Nishioka, K. Yoshino, D. Kuciauskas, and M.A. Scarpulla, *Appl. Phys. Exp.* 12, 081002 (2019).
 11. A. Chirilă, S. Buecheler, F. Pianezzi, P. Bloesch, C. Gretener, A.R. Uhl, C. Fella, L. Kranz, J. Perrenoud, S. Seyrling, R. Verma, S. Nishiwaki, Y.E. Romanyuk, G. Bilger, and A.N. Tiwari, *Nat. Mater.* 10, 857 (2011).
 12. S.H. Wei and A. Zunger, *Phys. Rev. B* 43, 1662 (1991).
 13. *Semiconductors: Basic Data* (Springer, Berlin, 1982), 2nd ed.
 14. S.H. Wei, S.B. Zhang, and A. Zunger, *J. Appl. Phys.* 87, 1304 (2000).
 15. B.E. McCandless, G.M. Hanket, D.G. Jensen, and R.W. Birkmire, *J. Vac. Sci. Technol., A* 20, 1462 (2002).
 16. N.R. Paudel and Y. Yan, *Appl. Phys. Lett.* 105, 183510 (2014).
 17. J.D. Poplawsky, W. Guo, N. Paudel, A. Ng, K. More, D. Leonard, and Y. Yan, *Nat. Commun.* 7, 12537 (2016).
 18. T.A.M. Fiducia, B.G. Mendis, K. Li, C.R.M. Grovenor, A.H. Munshi, K. Barth, W.S. Sampath, L.D. Wright, A. Abbas, J.W. Bowers, and J.M. Walls, *Nat. Energy* 4, 504 (2019).
 19. A. Nagaoka, K.B. Han, S. Misra, T. Wilenski, T.D. Sparks, and M.A. Scarpulla, *J. Crystal Growth* 467, 6 (2017).
 20. D. Kuciauskas, A. Kanevce, J.M. Burst, J.N. Duenow, R. Dhere, D.S. Albin, D.H. Levi, and R.K. Ahrenkiel, *IEEE J. Photovoltaics* 3, 1319 (2013).
 21. A.J. Strauss and J. Steininger, *J. Electrochem. Soc.* 117, 1420 (1970).
 22. T.A. Gessert, S.H. Wei, J. Ma, D.S. Albin, R.G. Dhere, J.N. Duenow, D. Kuciauskas, A. Kanevce, T.M. Barnes, J.M. Burst, W.L. Rance, M.O. Reese, and H.R. Moutinho, *Sol. Energy Mater. Sol. Cells* 119, 149 (2013).
 23. J.H. Yang, W.J. Yin, J.S. Park, W. Metzger, and S.H. Wei, *J. Appl. Phys.* 119, 045104 (2016).
 24. D. Kuciauskas, J.M. Kephart, J. Moseley, W.K. Metzger, W.S. Sampath, and P. Dippo, *Appl. Phys. Lett.* 112, 263901 (2018).
 25. C.H. Swartz, M. Edirisooriya, E.G. LeBlanc, O.C. Noriega, P.A.R.D. Jayathilaka, O.S. Ogedengbe, B.L. Hancock, M. Holtz, T.H. Myers, and K.N. Zaunbrecher, *Appl. Phys. Lett.* 105, 222107 (2014).
 26. J.H. Yang, L. Shi, L.W. Wang, and S.-H. Wei, *Sci. Rep.* 6, 21712 (2016).
 27. D. Kuciauskas, P. Dippo, A. Kanevce, Z. Zhao, L. Cheng, A. Los, M. Gloeckler, and W.K. Metzger, *Appl. Phys. Lett.* 107, 243906 (2015).

Publisher's Note Springer Nature remains neutral with regard to jurisdictional claims in published maps and institutional affiliations.